ON THE DISPUTED $\pi_1(1600)$ RESONANCE AND OBSERVATION OF A NEW ISO-VECTOR RESONANCE

F. Nerling[1][†]

on behalf of the COMPASS collaboration

(1) *Institut für Kernphysik, Universität Mainz, Becherweg 45, 55099 Mainz, Germany*
† E-mail: nerling@cern.ch

Abstract

The COMPASS experiment at CERN delivers new results on the search for exotic mesons. A spin-exotic resonance, the $\pi_1(1600)$, was reported by several experiments in the past. Those observations are, however, still to date highly disputed in the community. Especially the $\rho\pi$ decay channel allows for simultaneous observation of well established and less known resonances in different decay modes. The results from amplitude analysis of diffractively produced $(3\pi)^-$ final states show consistently a spin-exotic signal, that appears in agreement previous observations of the $\pi_1(1600)$. The high-statistics 2008 data sample allows and demands for an extended amplitude analysis method that further disentangles resonant and non-resonant particle production. The present status of analysis of COMPASS data and the observation of a new iso-vector meson $a_1(1420)$ is discussed.

Introduction

Exotic mesons have been reported by different experiments and in different decay channels. Quantum Chromodynamics (QCD) allows for and predicts exotic mesons like glue-balls, hybrids or tetraquarks according to several models. The experimental observation of so-called spin-exotic mesons, like the $\pi_1(1600)$ having exotic J^{PC} quantum numbers not accessible within the naive Constituent Quark Model, would be a fundamental confirmation of QCD, for a recent overview see e.g. [1]. Especially the resonant nature of signals observed in the exotic $J^{PC} = 1^{-+}$ partial-wave of the $\rho\pi$ decay channel, accessible via 3π final states, as reported by the E852/BNL and the VES experiments [2,3] in $\pi^-\pi^+\pi^-$ final states are questioned. The conclusions were withdrawn in later publications [4] and re-analyses of the $(3\pi)^-$ system in two decay modes (charged: $\pi^-\pi^+\pi^-$ and neutral: $\pi^-\pi^0\pi^0$) led to opposite conclusions [5]. One may get a hint at this controversy looking at [6].

The data taken with the COMPASS experiment at the CERN SPS provide excellent opportunity for the search for exotic resonances. In the 2004 pilot run data (π^- beam, Pb target), a significant J^{PC} spin-exotic signal at $1660\pm10^{+0}_{-64}\,\mathrm{MeV/c^2}$ is observed that is consistent with the disputed $\pi_1(1600)$; it shows a clean phase motion against well-known resonances [7]. The high statistics of the 2008 proton target data allows the search for exotic states in different decay modes in the same experiment, cf. [8]. Employing the same PWA analysis method as in [7], the results obtained for the $J^{PC}M^\epsilon=(1^{-+})1^+\rho^-\pi^0$ and $(1^{-+})1^+\rho^0\pi^-$ intensity and relative phase are similar to the previous observations [9, 10]. Apart of the established resonances $a_1(1260)$, $a_2(1320)$, $\pi_2(1670)$, also $\pi(1800)$ and $a_4(2040)$, an exotic signal in the 1^{-+} wave at around $1.6\,\mathrm{GeV/c^2}$ is observed, that shows a clean phase motion with respect to well-known resonances. These results are consistently obtained for both $\rho\pi$ decay modes, neutral and charged.
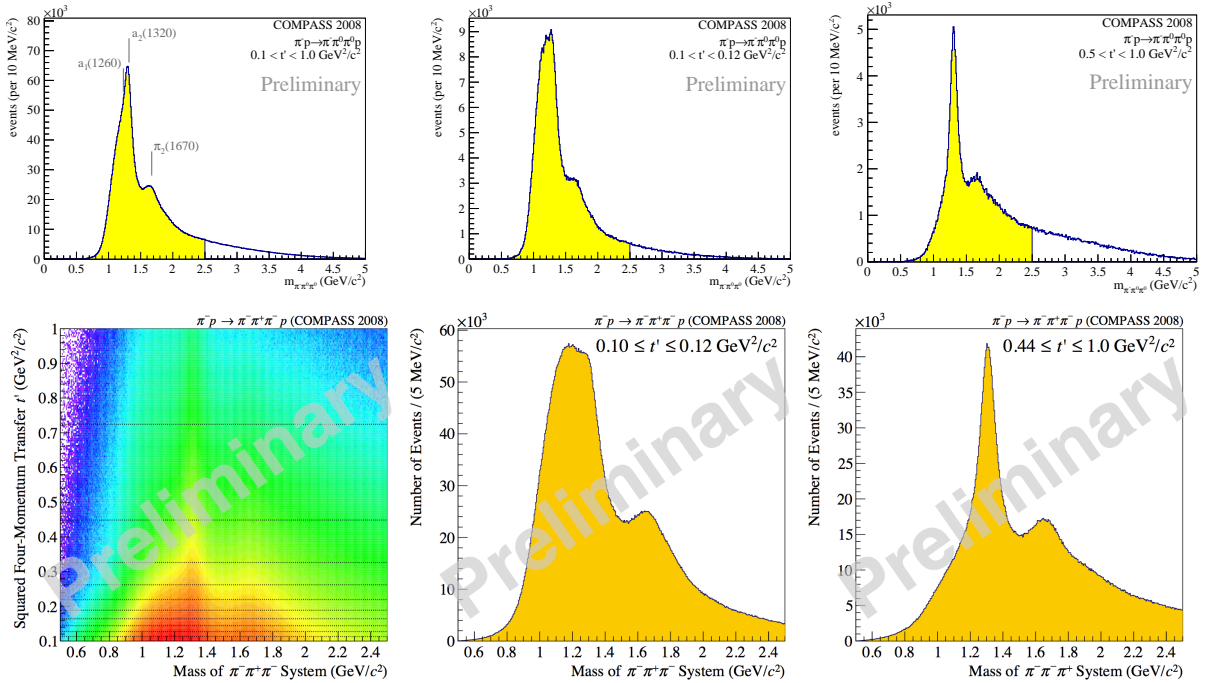
Figure 1: Mass spectra of the $(3\pi)^-$ systems. *Top: Neutral mode* — Different regions of momentum transfer t': "whole t'" *(left)*, "low t'" *(centre)* and "high t'"*(right)*. *Bottom: Charged mode* — Correlation of $m_{3\pi}$ and t' *(left)*, "low t'" *(centre)* and "high t'" *(right)*

New Partial-Wave Analysis Results

The data analysed for both $(3\pi)^-$ decay modes has been extended to the full 2008 proton target data. The total outgoing 3π-mass spectrum is shown for the neutral mode data in Fig. 1 (top) for the whole range of momentum transfer t' (Fig. 1, top, left), and for ranges of "low" and "high" (Fig. 1, top, centre and right) t' values, indicating a dependence of $m_{3\pi}$ on t'. This dependence is shown for the charged data (Fig. 1, bottom) at its whole glance in terms of a 2D plot of t' vs. $m_{3\pi}$ (Fig. 1, bottom, left). The two exemplary $m_{3\pi}$ spectra for the "low" and "high" t' values similar to the ones shown for the neutral mode (Fig. 1, top, centre and right) are given for comparison for the charged mode (Fig. 1, bottom, centre and right) as well, illustrating the similarity of the t' dependence observed for both, neutral and charged mode data.

Given the observed dependence on t' and the large statistics ($\sim 50\,\mathrm{M}\ \pi^-\pi^+\pi^-$, $\sim 3.5\,\mathrm{M}$ $\pi^-\pi^0\pi^0$ events), the partial-wave analysis (PWA) method has been extended w.r.t. to the previous scheme of a two-step PWA as applied previously [7, 9]. The first step analysis, the mass-independent PWA, has now been performed in different ranges of t' (a scheme already addressed in [5, 11]) with equal statistics contained in each bin, which is then completed by the second step mass-dependent Breit-Wigner χ^2 fit, that takes into account the observed t' dependencies by performing a simultaneous optimisation of the resonant parameters in all t' regions. This procedure disentangles resonant from non-resonant particle production (e.g. dynamically produced components caused by the Deck effect [12]), the former should not depend on t', whereas non-resonant backgrounds may well do so.

For the results presented here, the data has been divided into 8 and 11 bins of t' for the neutral and charged mode data, respectively, as illustrated for the charged data in Fig. 1 (bottom, left). The mass-independent PWA has been performed for each of the 8 and 11 ranges of t', whereas $40\,\mathrm{MeV}/c^2$ (neutral mode) and $20\,\mathrm{MeV}/c^2$ (charged mode)
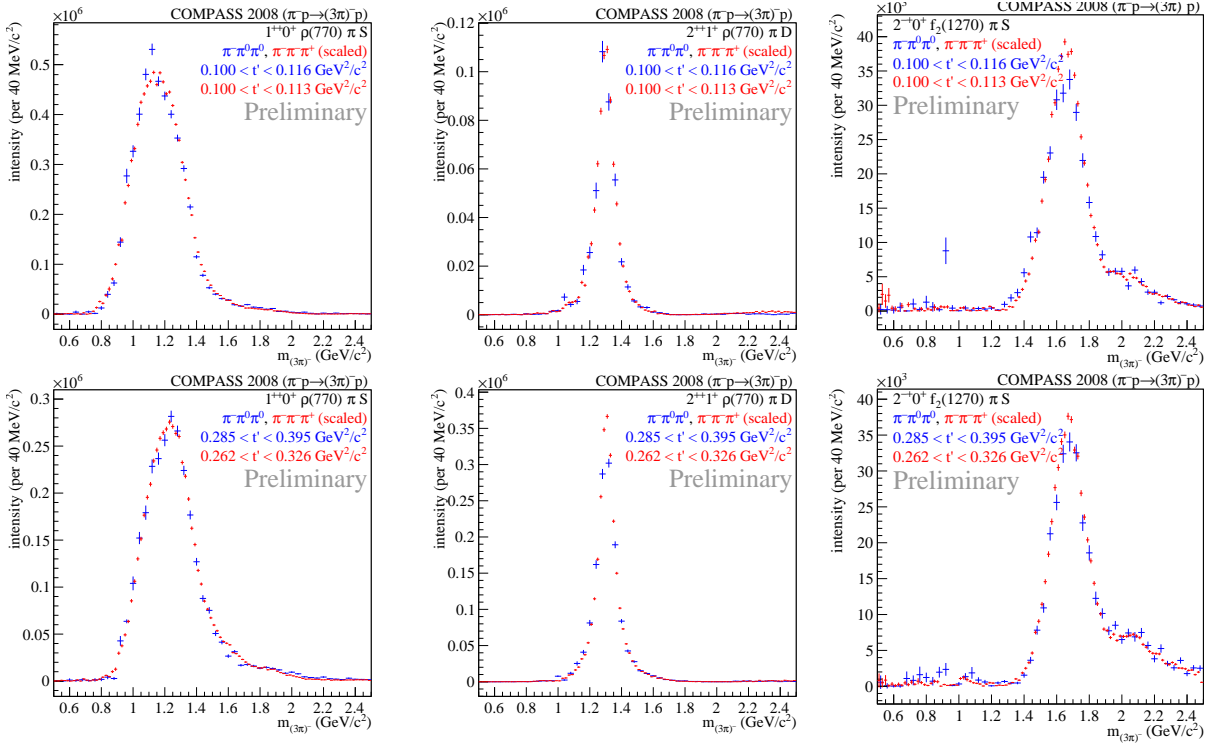
Figure 2: Mass-independent PWA result for neutral (blue) vs. charged (red) mode shown for the major waves for "low" *(top)* and "high" *(bottom)* values of t'. The $a_1(1260)$ in the $(1^{++})0^+\rho(770)\pi$ S-wave *(left)*, the $a_2(1320)$ in the $(2^{++})1^+\rho(770)\pi$ D-wave *(centre)* and the $\pi_2(1670)$ in the $(2^{-+})0^+f_2(1270)\pi$ S-wave *(right)* are shown.

wide $m_{3\pi}$ bins have been chosen as previously [9, 10]. The wave-set has been extended from 53 to 88 partial-waves. The mass-dependent PWA including 6 out of the 88 waves is released for public merely for the charged mode data, see also [13, 14] for more details.

In Fig. 2, the mass-independently fitted intensities for the major waves are shown for exemplary two very different ranges of t' ("low" and "high") for both, the neutral and the charged mode fit results (normalised to the integral for each plot to compare the shapes). The main resonances $a_1(1260)$ (Fig. 2, left), $a_2(1320)$ (Fig. 2, centre), and $\pi_2(1670)$ (Fig. 2, right) are consistently observed for the neutral vs. charged mode data, the shapes are mostly coinciding for the different t' ranges "low" and "high" (Fig. 2, top and bottom). While the $a_2(1320)$ and $\pi_2(1670)$ (Fig. 2, centre and right) are observed rather robust in shape against t', the $a_1(1260)$ (Fig. 2, left) shows a significant shift in mass for the different t'. In addition, structures around the $a_1(1260)$ and $\pi_2(1670)$ (Fig. 2, left and right) reveal underlying dynamics resulting in a t' dependent shape, which cannot be solely attributed to a resonance. This will be resolved by the completing second step, the mass-dependent fit. Fitting the Breit-Wigner description of the resonances simultaneously to the different t' ranges, while allowing for background contributions, indeed different relative contributions of non-resonant background are found, depending on t' (Fig. 3).

Summing incoherently up the mass-independently fitted intensities of all t' bins, one obtains a similar result as obtained previously [9], where the mass-independent PWA were performed in bins of $m_{3\pi}$ only. The intensity spectra obtained with the extended method discussed here are basically smoother, as the t' dependence is taken into account directly from the data instead of using the t' slopes for the various resonances parameterised from the data. For the three main waves, in which we observe the $a_1(1260)$, the $a_2(1320)$ and
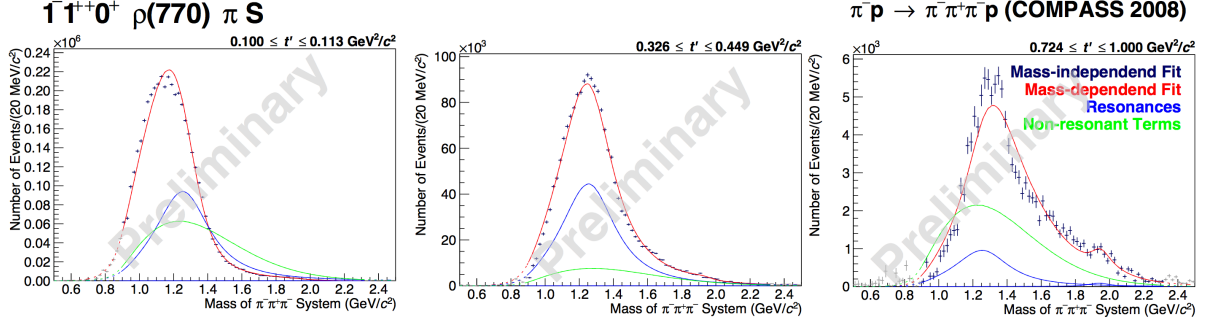
Figure 3: Complete PWA result for the $(1^{++})0^+\rho(770)\pi$ S-wave, in which we observe the $a_1(1260)$, shown for three exemplary bins in t' ("low", "medium", and "high"). Shown are the mass-independent fit result (data points) and overlaid the fitted Breit-Wigner (BW) description (red curve), which consists of the BW describing the $a_1(1260)$ (blue curve) and the non-resonant background contribution (green curve).

the $\pi_2(1670)$, shown for different t' ranges in Fig. 2, the incoherent sums of intensities over all t' ranges are shown in Fig. 4 (top) for each wave. Further incoherent sums are presented for the $(0^{-+})0^+f_0(980)\pi$ S-wave and the $(4^{++})1^+\rho(770)\pi$ S-wave (Fig. 4, bottom, left and centre), showing the $\pi(1800)$ and $a_4(2040)$, respectively, and the $(0^{-+})0^+(\pi\pi)_s\pi$ S-wave (Fig. 4, bottom, right), where the peak at around $1.8\,\mathrm{GeV}/c^2$ can be attributed to the $\pi(1800)$. Other experiments claimed also a $\pi(1300)$ — the object at the mass between 1 and $1.4\,\mathrm{GeV}/c^2$ in the $(0^{-+})0^+(\pi\pi)_s\pi$ S-wave shows some differences for the neutral vs. the charged mode COMPASS data.
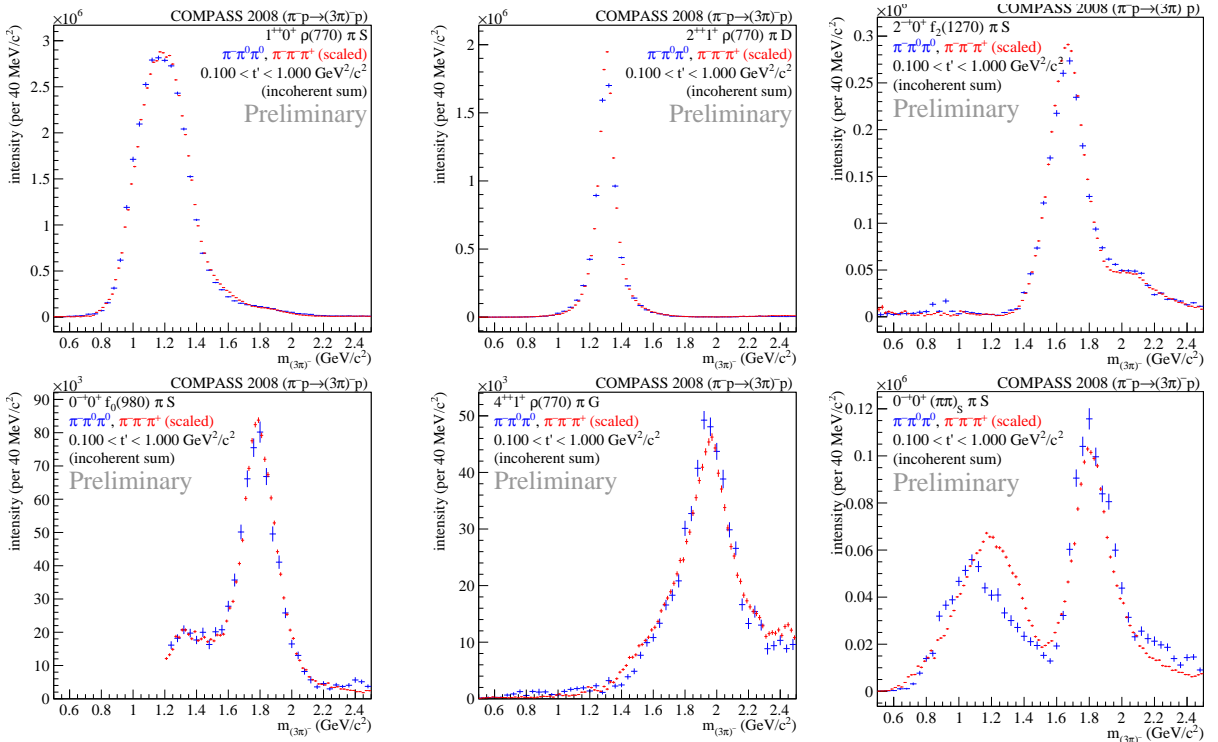

Figure 4: Incoherent sum over the different t' ranges of mass-independently fitted intensities of major and smaller waves compared for neutral (blue) and charged (red) mode data. Shown are the three major waves (cf. also Fig. 2) *(top)* and those, in which the $\pi(1800)$ *(bottom, left and right)* and the $a_4(2040)$ *(bottom, centre)* are observed.
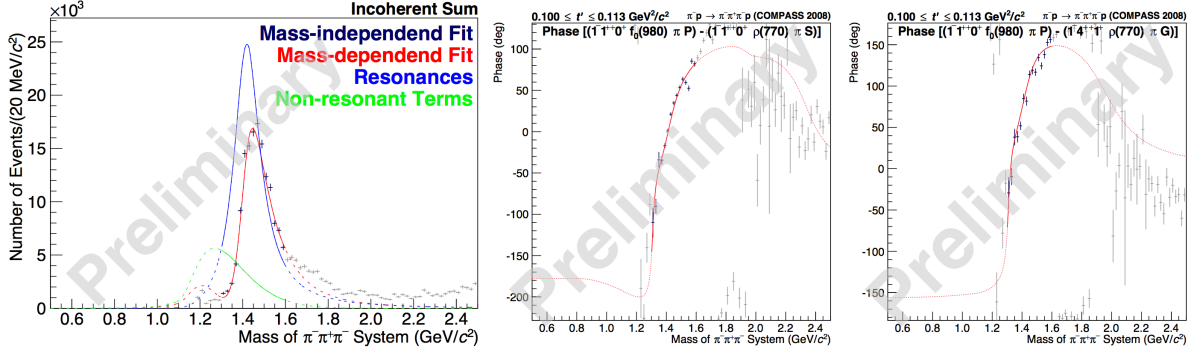
Figure 5: PWA result for the $(1^{++})0^+ f_0(980)\pi$ P-wave. The mass-independently fitted intensities for the neutral and the charged mode data show a narrow structure at $1420\,\text{MeV}/c^2$ (first presented in [14] and [13]). For the charged mode data, the mass-independent fit result is shown (data points) with the fitted BW description (red curve) overlaid, which consists of the BW describing the object at $1420\,\text{MeV}/c^2$ (blue curve) and the non-resonant background contribution (green curve) (left). The corresponding relative phases w.r.t. two other waves are shown, again the mass-independent result (data points) with the mass-dependent fit result overlaid (black line) (centre and right).

The PWA results for the $(1^{++})0^+ f_0(980)\pi$ P-wave in the charged mode data are displayed in Fig. 5. The mass-independently fitted intensities (incoherent sums of the different t' ranges) are shown (Fig. 5, left). The data exhibits, even though low in intensity, a strong enhancement in form of a clean narrow peak at $1420\,\text{MeV}/c^2$, that is consistently observed for the neutral and the charged mode data, see also [14] and [13], respectively. The mass-independent PWA completed by the simultaneous BW fit to the result obtained from the mass-independent fit performed in the different ranges of t' is shown for the $(1^{++})0^+ f_0(980)\pi$ P-wave in the charged mode data in Fig. 5 (left). Here, the result of the mass-dependent fit is overlaid (curves) in addition. It consists of a BW describing the narrow object and some non-resonant component. No such object has previously been observed.

The relative phases of this object observed in the $(1^{++})0^+ f_0(980)\pi$ P-wave against the $a_1(1260)$ in the $(1^{++})0^+ \rho(770)\pi$ S-wave and the $a_4(2040)$ in the $(4^{++})1^+ \rho(770)\pi$ G-wave are shown in Fig. 5 (centre and right), again with the mass-dependent fit result overlaid. A clean phase motion is observed exactly in the mass region of about 1.3-1.6 GeV/c^2, where the object is observed in the intensity plots, convincing that the object is of resonant nature.

The neutral and the charged mode results are consistent not only for the well and less established states, but also for this new iso-vector resonance, that we call $a_1(1420)$. The new $a_1(1420)$ decaying into $f_0(980)\pi$ (and not observed in $\rho\pi$) is produced at a rather low intensity (less than 0.25 % of the total intensity), which might hint to a large strangeness content and an exotic nature. Similarly to $a_0(980)$ and $f_0(980)$, it might be the isospin-1 partner of the $f_1(1420)$ (that we observe well resolved decaying to $K\bar{K}\pi$ [15]) strongly coupling to KK^*, at least the similarity in width and mass is striking.

Conclusions & Outlook

In summary, we extended our PWA method to disentangle contributions from resonant and non-resonant production. The neutral and the charged mode $(3\pi)^-$ data diffractively

produced on a proton target show consistent results concerning major and less known resonances. In particular, we observe a new possibly exotic iso-vector state $a_1(1420)$ decaying into $f_0(980)\pi$ (and not observed in $\rho\pi$), having a width of about $140 \, \text{MeV}/c^2$ and showing resonant behaviour. The analyses will be proceeded, including the extraction of the $(\pi\pi)_s$ wave subsystem (not discussed here), before stronger conclusions will be drawn also on the disputed $\pi_1(1600)$ resonance, for which the interpretation as a narrow (Γ=150-200 MeV) resonance is excluded, and thus its nature can (partly) be connected to dynamical effects on top of a non-resonating Deck-like amplitude.

References

[1] C.A. Meyer and Y.Van. Haarlem, Phys. Rev. C **82** (2010) 025208.

[2] G. S. Adams *et al.*, Phys. Rev. Lett. **81**, (1998) 5760.

[3] Y. Khokhlov, Nucl. Phys. **A663** (2000) 596.

[4] D. V. Amelin *et al.*, Phys. Atom. Nucl. **68** (2005) 359.

[5] A.R. Dzierba *et al.*, Phys. Rev. D **73** (2006) 072001.

[6] J. Beringer *et al.*, (Particle Data Group), Phys. Rev. D **86** (2012) 010001.

[7] M. Alekseev *et al.*, COMPASS collaboration, Phys. Rev. Lett, **104** (2010) 241803.

[8] F. Nerling, AIP Conf. Proc. **1257** (2010) 286; arXiv:1007.2951[hep-ex].

[9] F. Nerling, EPJ Web Conf. **37** (2012) 09025; arXiv:1208.0474[hep-ex].

[10] F. Haas, Conf. Proc., Hadron2011, Munich (2011); arXiv:1109.1789v2[hep-ex].

[11] C. Daum *et al.*, Phys. Lett. **89**B (1980) 276; Phys. Lett. **89**B (1980) 281.

[12] R.T. Deck, Phys. Rev. Lett. **13** (1964) 169.

[13] S. Paul, Conf. Proc., MENU 2013, Rom, Italy, (2013); arXiv:1312.3678[hep-ex].

[14] S. Uhl, Conf. Proc., Hadron2013, Nara, Japan, (2013); arXiv:1401.4943[hep-ex].

[15] J. Bernhard and F. Nerling, Conf. Proc. Hadron2011, Munich (2011); arXiv:1109.0219[hep-ex].